A POSTERIORI ERROR ESTIMATOR FOR HIERARCHICAL MODELS FOR ELASTIC BODIES WITH THIN DOMAIN

Jin Rae Cho*
Research Institute of Mechanical Technology
Pusan National University, Pusan 609-735, Korea

and

J. Tinsley Oden**
Texas Institute for Computational and Applied Mathematics
The University of Texas at Austin, Austin, Tx 78712, USA

Abstract

A concept of hierarchical modeling, the newest modeling technology, has been introduced early in 1990. This new technology has a great potential to advance the capabilities of current computational mechanics. A first step to implement this concept is to construct hierarchical models, a family of mathematical models which are sequentially connected by a key parameter of the problem under consideration and have different levels in modeling accuracy, and to investigate characteristics in their numerical simulation aspects.

Among representative model problems to explore this concept are elastic structures such as beam-, arch-, plate- and shell-like structures because the mechanical behavior through the thickness can be approximated with sequential accuracy by varying the order of thickness polynomials in the displacement or stress fields.

But, in the numerical analysis of hierarchical models, two kinds of errors prevail; the modeling error and the numerical approximation error. To ensure numerical simulation quality, an accurate estimation of these two errors is definitely essential.

Here, a local *a posteriori* error estimator for elastic structures with thin domain such as plate- and shell-like structures is derived using element residuals and flux balancing technique. This method guarantees upper bounds for the global error, and also provides accurate local error indicators for two types of errors, in the energy norm. Comparing to the classical error estimators using flux averaging technique, this shows considerably reliable and accurate effectivity indices.

To illustrate the theoretical results and to verify the validity of the proposed error estimator, representative numerical examples are provided.

Key Words : Hierarchical model, Elastic body, *A posteriori* error estimator, Flux balancing, Effectivity index

Introduction

In every numerical analysis of natural phenomena using hierarchical models, at least two types of errors prevail:

(i) The error inherent in the hierarchical model itself due to assumptions made on it which may make it insufficient to depict significant complicated features of the behavior.

(ii) The numerical error in the numerical approximation of the solution corresponding to a particular hierarchical model.

* : Assistant Professor, School of Mechanical Engineering (jrcho@hyowon.pusan.ac.kr)
** : Chair Professor, Aerospace Engineering and Engineering Mechanics, and Director of TICAM

To the best of my memory, the mathematical derivation of a priori modeling error estimate for one-dimensional elliptic boundary value problems of scalar-valued functions was made by Vogelius and Babuska(1981). And recently, its extension to two- and three-dimensional linear elasticity problems with thin domain was done by the authors(1996a). As for a priori error estimation of finite element approximations for elastic bodies with thin domain, the authors(1996b) have developed including the locking effect, and found that two types of errors are orthogonal in the energy norm sense.

Schwab(1996) developed one simple a posteriori modeling error estimator for hierarchical models for plate-like structures using an introduction of the decomposition in modeling error and the use of traction residuals on the top and bottom surfaces of such structures.

This paper is concerned with a development of a posteriori error estimator which can estimate accurately the total error due to two types of errors, that is one measured with respect to the fully linear elasticity theory. A reliable and efficient error estimator is an essential tool for selecting optimal hierarchical model and its optimal finite element mesh.

Here, we use the mathematical theory advanced by Ainsworth and Oden(1993). This involves the use of localized element residuals and equilibrated flux splitting to produce upper bounds for the global error in the energy norm. The implementation of this error estimator is composed of four steps:

(1) We perform a finite element analysis with a setting of initial model level (q_0) and initial finite element mesh (h_0, p_0).

(2) We then calculate equilibrated flux on each interelement boundary from the solutions obtained in step (1).

(3) Next, we solve the local equilibrated problem for each element with higher model level q and higher approximation order p than those in the initial setting.

(4) Finally we calculate local error indicators for each element using the two solutions obtained steps (1) and (3).

Error indicators estimated with this error estimator enable one to assess the validity of a specified hierarchical model as well as a specified finite element mesh for thin elastic bodies such as beam-, arch, plate- and shell-like structures.

Preliminaries

Let Ω be an open Lipschitzian domain in $\mathbb{R}^3$ with piecewise smooth boundary $\partial\Omega$. The Sobolev space $H^m(\Omega)$, m =non-negative integers, is a Hilbert space defined as the completion of $\{ u \in C^m(\Omega) : \|u\|_{m,\Omega} < \infty \}$ in the Sobolev norm defined as

$$\|u\|_{m,\Omega} = \left\{ \sum_{|\alpha| \le m} \int_\Omega | D^\alpha u|^2 d\Omega \right\}^{1/2} \tag{1}$$

where multi-index notation is used: $\alpha = (\alpha_1, \alpha_2, \alpha_3)$, $\alpha_i \in \geq 0$, $|\alpha| = \alpha_1 + \alpha_2 + \alpha_3$ and Eq. (2) defines

$$D^\alpha u = \frac{\partial^{|\alpha|} u}{\partial x_1^{\alpha_1} \partial x_2^{\alpha_2} \partial x_3^{\alpha_3}} \tag{2}$$

weak or distributional partial derivatives. The inner product in the space $H^m(\Omega)$ is defined as follows:

$$(u, v)_{m,\Omega} = \sum_{|\alpha|, |\beta| \le m} \int_\Omega D^\alpha u \cdot D^\beta v \, d\Omega \tag{3}$$

Furthermore, $H_0^m(\Omega)$ is defined as the closure of $C_0^\infty(\Omega)$ in the space $H^m(\Omega)$. More mathematical

details on the definition may be referred to Adams(1978).

Next, we introduce some useful notations concerning with the finite element partition, and which are used in the derivation of a posteriori error estimator. Let $\wp$ be a partition of Ω into a collection of $N = N(\wp)$ subdomains Ω_K with boundaries $\partial\Omega_K$ such that

i) $N(\wp) < \infty$

ii) Ω_K is Lipschitzian with piecewise smooth boundary $\partial\Omega_K$

iii) $\overline{\Omega} = \bigcup_{K=1}^{N} \overline{\Omega}_K$, $\Omega_K \cap \Omega_L = \emptyset$, $K \neq L$

iv) $\overline{\Omega}_K \cap \overline{\Omega}_L$ is either empty or common line or common smooth surface Γ_{KL}

Here, $\boldsymbol{n}_K$ be the outward unit normal vector on the element Ω_K, then $\boldsymbol{n}(s)$ on Γ_{KL} is defined by

$$\begin{aligned} \boldsymbol{n}(s) &= \aleph_{KL}\boldsymbol{n}_K(s) = \aleph_{LK}\boldsymbol{n}_L(s) \\ \aleph_{KL} &= -\aleph_{LK} = \begin{cases} 1 & \text{if } K > L \\ -1 & \text{if } K < L \end{cases} \end{aligned} \tag{4}$$

and which implies $\boldsymbol{n}(s) = \boldsymbol{n}_K(s)$, $s \in \partial\Omega_K$: K is a larger element number. In addition, we define the jump $[\![v]\!]$ of functions v across the interelement boundary Γ_{KL} of elements Ω_K, Ω_L. Futhermore,

$$[\![\boldsymbol{v}]\!] = \begin{cases} \boldsymbol{v}_K - \boldsymbol{v}_L & \text{if } K > L \\ \boldsymbol{v}_L - \boldsymbol{v}_K & \text{if } K < L \end{cases} \tag{5}$$

we will denote i-component of traction vector t due to Cauchy stress tensor $\sigma(u)$ using the operator Γ.

$$t_i = \sigma_{ji} n_j = \langle \Gamma(\boldsymbol{n})\, \sigma(\boldsymbol{u}) \rangle^i \tag{6}$$

Formulation of Hierarchical Models

Variational Formulation

For a purpose of notations, let us consider a plate-like structure with uniform thickness d, as shown in Fig. 1. Let $\omega \subset R^2$ denote an open bounded region (mid-surface) of the body $\Omega \subset R^3$

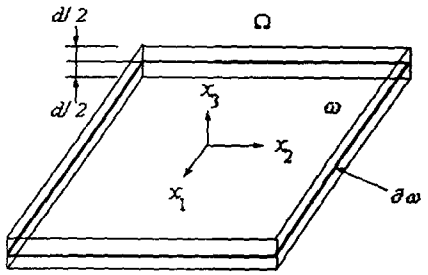

Fig. 1 A plate-like structure and its geometric notations

with piecewise smooth boundary $\partial\omega$. For the boundary of the body, we denote the lateral boundary and the top and bottom surfaces of the body by $\partial\Omega_\ell$, $\partial\Omega_\pm$, respectively:

$$\begin{aligned} \partial\Omega_\ell &= \{\, x \in R^3 \mid (x_1, x_2) \in \partial\omega,\ |x_3| < d/2 \,\} \\ \partial\Omega_\pm &= \{\, x \in R^3 \mid (x_1, x_2) \in \partial\omega,\ |x_3| = d/2 \,\} \\ \partial\Omega &= \overline{\partial\Omega_\ell \cup \partial\Omega_\pm} \end{aligned} \tag{7}$$

Here, x_3 is a coordinate normal to the reference surface ω. Further, let Γ_D and Γ_N be the portions of the boundary $\partial\Omega$ such that $\overline{\Gamma_D \cup \Gamma_N} = \partial\Omega$, $\Gamma_D \cap \Gamma_N = \emptyset$, on which the displacements and the applied tractions are specified (i.e., Dirichlet and Neumann boundary regions), respectively. Usually, Γ_D is restricted to the lateral boundary and Γ_N being to the top and bottom surfaces. For convenience of notations, let us define $\partial\omega_D$, $\partial\omega_N$ by

$$\begin{aligned} \partial\omega_D &= \{\, x \in \Gamma_D \mid x_3 = 0 \,\} \\ \partial\omega_N &= \{(x_1, x_2, 0) \in \omega \mid (x_1, x_2, \pm d/2) \in \Gamma_N\} \end{aligned} \tag{8}$$

Viewing as a three-dimensional elastic body (as opposed to plate or shell), governing equations are written in the following elliptic boundary value problems,

$$\begin{aligned} -D^T \sigma(u) &= f, \quad \text{in } \Omega \\ u &= 0, \quad \text{on } \Gamma_D \\ \Gamma(n)\, \sigma(u) &= t, \quad \text{on } \Gamma_N \end{aligned} \tag{9}$$

and the strain-displacement relations and the constitutive equations are expressed as follows:

$$\begin{aligned} \varepsilon(u) &= D u \\ \sigma(u) &= E D u \end{aligned} \tag{10}$$

Here, D^T denotes divergence-like operator in the cartesian coordinate system and ε, σ are vectors of Cauchy strains and stresses; $\sigma = \{\varepsilon_1, \varepsilon_2, \varepsilon_3, \gamma_{12}, \gamma_{23}, \gamma_{31}\}^T$, $\sigma = \{\sigma_1, \sigma_2, \sigma_3, \tau_{12}, \tau_{23}, \tau_{31}\}^T$. And n is the unit outward normal at the boundary $\partial\Omega$,

$$D^T = \begin{bmatrix} \partial/\partial x_1 & 0 & 0 & \partial/\partial x_2 & 0 & \partial/\partial x_3 \\ 0 & \partial/\partial x_2 & 0 & \partial/\partial x_1 & \partial/\partial x_3 & 0 \\ 0 & 0 & \partial/\partial x_3 & 0 & \partial/\partial x_2 & \partial/\partial x_1 \end{bmatrix} \tag{11}$$

while $\mathbf{f} \in [L^2(\Omega)]^3$, $\mathbf{t} \in [L^2(\Gamma_N)]^3$, respectively, represent body force and applied traction vectors. E is (6 x 6) matrix containing Lame constants μ, λ for linear elastic materials (Szabo and Babuska (1991)).

We define the space $V(\Omega)$ by $\{ \mathbf{v}(\mathbf{x}) \in [H^1(\Omega)]^3 : \mathbf{v} = \mathbf{0} \text{ on } \Gamma_D\}$, then this space is admissible displacement space for the elliptic boundary value problem of Eq. (9) because every vector-valued function $\mathbf{v} \in V(\Omega)$ satisfies homogeneous boundary conditions on Γ_D and has finite strain energy $U(\mathbf{v})$:

$$\begin{aligned} U(\boldsymbol{v}) &= \frac{1}{2}\int_\Omega \varepsilon(\boldsymbol{v}) : \sigma(\boldsymbol{v})\, d\Omega \\ &= \frac{1}{2}\int_\Omega (\boldsymbol{D}\,\boldsymbol{v})^T (\boldsymbol{E}\,\boldsymbol{D}\,\boldsymbol{v})\, d\Omega \end{aligned} \tag{12}$$

Now, let q be (q_1, q_2, q_3) with q_i being non-negative integers, and define the function space $V(\omega)$ defined on the mid-surface by

$$V(\omega) = \{ v(x_1, x_2) : v \in H^1(\omega) \mid v = 0 \text{ on } \partial\omega_N\} \tag{13}$$

Next, we define the subspace $V^q(\Omega) \subset V(\Omega)$ by introducing a set of Legendre polynomials $\Psi_\ell(x_3)$ and by specifying a set of their maximum orders (q_1, q_2, q_3).

$$V^q(\Omega) = \left\{ \boldsymbol{v}(\boldsymbol{x}) \mid v_i = \sum_{\ell=0}^{q_i} \Theta_i^\ell(x_1, x_2) \cdot \Psi_\ell(2x_3/d),\ \Theta_i^\ell \in V(\omega),\ i = 1,2,3 \right\} \tag{14}$$

Then, from the density argument (Adams(1978)), $V^q(\Omega) \hookrightarrow V(\Omega)$ as $q \to \infty$.

The space $V^q(\Omega)$ is a restricted subspace of $V(\Omega)$ with finite dimension in the thickness variation in displacement fields. In this subspace, Galerkin weighed residual method for the three-dimensional linear elasticity is expressed as following statement:

$$\begin{aligned} &\text{Find } \mathbf{u}^q \in V^q(\Omega) \text{ such that } \forall\, \mathbf{v}^q \in V^q(\Omega) \\ &\qquad a(\boldsymbol{u}^q, \boldsymbol{v}^q) = \ell(\boldsymbol{v}^q) \end{aligned} \tag{15}$$

Where, the bilinear functional $a(\cdot, \cdot) : V^q(\Omega) \times V^q(\Omega) \to R$ and the linear functional $\ell(\cdot) : V^q(\Omega) \to R$ are expressed by the following dimensionally-reduced form defined on the mid-surface, respectively:

$$\begin{aligned} a(\boldsymbol{u}^q, \boldsymbol{v}^q) &= \int_\omega \left\{ \int_{-d/2}^{d/2} (\boldsymbol{D}\,\boldsymbol{v}^q)^T (\boldsymbol{E}\boldsymbol{D}\,\boldsymbol{u}^q)\, dx_3 \right\} d\omega \\ \ell(\boldsymbol{v}^q) &= \int_\omega \left\{ \int_{d/2}^{d/2} f^T \boldsymbol{v}^q\, dx_3 \right\} d\omega + \int_{\partial\omega_N} \{ \boldsymbol{t}^{+T} \boldsymbol{v}^q(\omega, d/2) + \boldsymbol{t}^{-T} \boldsymbol{v}^q(\omega, -d/2) \}\, d\omega \end{aligned} \tag{16}$$

Obviously, the variational problem (15) is two dimensional because integrations through the thickness are solely related to the thickness polynomials $\Psi_\ell(x_3)$, as shown in Eq. (16).

The solution u^q of (15) is defined as a projection of u in the bilinear functional, i.e., $a(u - u^q, v) = 0, \forall v \in V^q(\Omega)$. We can construct a sequential set $\{u^q\}_{q=0}^{\infty}$ of solution according to different sets of (q_1, q_2, q_3). We define this set as hierarchical models and denote by

$$F_H = \{ u^q : q = 0, 1, \cdot, \cdot, \cdot, \infty \} \tag{17}$$

This hierarchical family is constructed by sequentially specifying the order(the model level) q. Hereafter, we will denote a hierarchical model with the model level (q_1, q_2, q_3) as the (q_1, q_2, q_3) model. Their characteristics are well explained in the work of Babuska and Li(1992), Szabo and Babuska(1991), Cho and Oden(1996a, 1996b), Oden and Cho(1996) and Schwab(1996). We record here that $(q_1, q_2, q_3)^*$ models represent hierarchical models constructed by replacing E with E^{RM}, material moduli being used in the Reissner-Mindlin theory.

Finite Element Approximation

The restriction of the test function v to Ω_K belongs to the space $V_K^q(\Omega_K)$ denoted by

$$V_K^q = \{ v_K^q \mid v_K^q = v^q|_{\Omega_K} \} \tag{18}$$

Let be v_K^q a local finite element approximation obtained using approximation polynomials of order p_K defined on the mid-surface. Since the global finite element approximation $v^{q,h}$ should be continuous at the interelement boundaries for producing finite energy, the global finite element approximation $V^{q,h}(\Omega)$ contains vector-valued test functions such that

$$v^{q,h} \in [C^0(\overline{\Omega})]^3, \quad \forall\, v^{q,h} \in V^{q,h}(\Omega) \tag{19}$$

Then, the finite element approximation for the (q_1, q_2, q_3) hierarchical model is as follows:

$$\text{Find} \quad v^{q,h} \in V^{q,h}(\Omega) \text{ such that } \forall\, v^{q,h} \in V^{q,h}(\Omega)$$
$$a(u^{q,h}, v^{q,h}) = \ell(v^{q,h}) \tag{20}$$

Since the assumed admissible displacement fields are in the form of Eq. (14), finite element approximation is to find approximate solutions $\Theta_i^{\ell,h}(x_1, x_2)$ corresponding to each thickness polynomial order using two-dimensional basis functions $\{\phi_k(x_1, x_2)\}$ so that

$$\Theta_i^{\ell,h}(x_1, x_2) = \sum_{k=0} \overline{\Theta}_{i,k}^{\ell,h} \cdot \phi_k(x_1, x_2) \tag{21}$$

Clearly, at each finite element node, $(q_1 + q_2 + q_3 + 3)$ degrees of freedom $\{\overline{\Theta}_{i,k}^{\ell,h}\}_{\ell=0}^{q_i}$ are assigned.

A Posteriori Error Estimation

Upper Bound and Local Error Indicators

Let $\mathbf{u}$ and $\mathbf{u}^q$ be the exact (three dimensional elasticity theory) and the hierarchical model with a model level $\mathbf{q}=\{q_1,q_2,q_3\}$, respectively. Then, the modeling error $\mathbf{e}^q \in \mathrm{V}(\Omega)$ of the hierarchical model is defined as $\mathbf{e}^q = \mathbf{u} - \mathbf{u}^q$. And let $\mathbf{u}^{q,h}$ be the solution of the finite element approximation for the hierarchical model, then its finite element approximation error $\mathbf{e}^{q,h} \in \mathrm{V}^q(\Omega)$ is denoted by $\mathbf{e}^{q,h} = \mathbf{u}^q - \mathbf{u}^{q,h}$. Combining these two errors, we can define the finite element approximation error $\mathbf{e}$ measured with respect to the exact solution:

$$e \in V(\Omega), \quad e = e^q + e^{q,h} = u - u^{q,h} \tag{22}$$

The energy norm $\|\cdot\|_E$ is defined using the bilinear functional $a(\cdot,\cdot)$ in Eq. (16). And let

$$\|v\|_E = \sqrt{a(v,v)} \tag{23}$$

the linear functionals $\Pi : \mathrm{V}(\Omega) \to \mathrm{R}$, $\Pi_q : \mathrm{V}^q \to \mathrm{R}$ and $J : \mathrm{V}(\Omega) \to \mathrm{R}$ be defined as, respectively

$$\begin{aligned} \Pi(v) &= \frac{1}{2}a(v,v) - \ell(v) \\ \Pi_q(v) &= \frac{1}{2}a(v^q, v^q) - \ell(v^q) \\ J(v) &= \Pi(v) - \Pi_q(u^{q,h}) \end{aligned} \tag{24}$$

Next, consider a difference between the two potential functionals $\Pi(u)$ and $\Pi_q(u^{q,h})$, where

$$\begin{aligned} J(u) &= \frac{1}{2}a(u,u) - \ell(u) - \frac{1}{2}a(u^{q,h}, u^{q,h}) + \ell(u^{q,h}) \\ &= -\frac{1}{2}a(u-u^{q,h}, u-u^{q,h}) - \ell(u) + \ell(u^{q,h}) \\ &\quad + a(u,u) - a(u,u^{q,h}) \end{aligned} \tag{25}$$

we use the fact that $a(\mathbf{u}^{q,h}, \mathbf{u}^{q,h})$ and $\ell(\mathbf{u}^{q,h})$ are restrictions from the space V into V^q, respectively. It is not difficult to prove that we have

$$-\frac{1}{2}\|e\|_E^2 = J(u) = \Pi(u) - \Pi_q(u^{q,h}) = \inf_{v \in V(\Omega)} \Pi(v) - \Pi_q(u^{q,h}) \tag{26}$$

We define the local solution spaces V_K and V_K^q in a subdomain Ω_K, and introduce two broken

$$\begin{aligned} V_K &= \{ v \in [H^1(\Omega_K)]^3 \mid v = 0 \text{ on } \partial\Omega_K \cap \Gamma_D \} \\ V_K^q &= V_K \cap V^q \end{aligned} \tag{27}$$

spaces as in Eq. (27). Then $\mathbf{v} \in \mathrm{V}(\mathcal{S})$ and $\mathrm{V}^q(\mathcal{S})$ are discontinuous across the interelement boundary

$$V(\mathcal{S}) = \prod_{K=1}^{N(\mathcal{S})} V_K, \quad V(\mathcal{S}) \supset V(\Omega), \qquad V^q(\mathcal{S}) = \prod_{K=1}^{N(\mathcal{S})} V_K^q, \quad V^q(\mathcal{S}) \supset V^q(\Omega) \tag{28}$$

Γ_{KL}. In the local spaces V_K, V_K^q, the bilinear and the linear functionals $a(\cdot,\cdot)$, $\ell(\cdot)$, Π restricted to a finite element are denoted by $a_{K(\cdot,\cdot)}$, $\ell_{K(\cdot)}$, Π_K, respectively.

We introduce the splitting function $\alpha_{KL}: \Gamma_{KL}(s) \to R$ on the interelement boundary $\Gamma_{KL}(s)$ as

$$\alpha^k_{KL}(s) + \alpha^k_{LK}(s) = 1, \quad k = 1,2,3 \tag{29}$$

With this splitting functions, we define the self-equilibrated k-component of traction acting on the element Ω_K along $\Gamma_{KL}(s)$ defined as

$$\langle \Gamma(n)\, \sigma(u^{q,h})\rangle^k_{1-\alpha} = \alpha^k_{LK}\langle \Gamma(n_K)\, \sigma(u^{q,h}_K)\rangle^k + \alpha^k_{KL}\langle \Gamma(n_K)\, \sigma(u^{q,h}_L)\rangle^k \tag{30}$$

Then, it can be easily verified the relation of Eq. (31) for every $v \in V^q(\wp)$. Next, we extend

$$\sum_{K=1}^{N(\wp)} \int_{\partial\Omega_K \setminus \partial\Omega} v^T \langle \Gamma(n)\, \sigma(u^{q,h})\rangle_{1-\alpha} ds = \sum_{\Gamma_{KL}} \int_{\Gamma_{KL}} [[\, v^T]] \langle \Gamma(n)\, \sigma(u^{q,h})\rangle_{1-\alpha} ds \tag{31}$$

Π to the spaces $V(\wp)$ and $V^q(\wp)$, respectively and consider the difference functional (potential functional) $J_\wp: V(\wp) \to R$.

$$\begin{aligned} J_\wp(v) &= \Pi(v) - \Pi(u^{q,h}), \quad v \in V(\wp) \\ &= \sum_{K=1}^{N(\wp)} \left\{ \Pi_K(v) - \Pi_K(u^{q,h}) - \int_{\partial\Omega_K \setminus \partial\Omega} v^T \langle \Gamma(n)\, \sigma(u^{q,h})\rangle_{1-\alpha} ds \right\} \\ &\quad + \sum_{\Gamma_{KL}} \int_{\Gamma_{KL}} [[\, v^T]] \langle \Gamma(n)\, \sigma(u^{q,h})\rangle_{1-\alpha} ds \end{aligned} \tag{32}$$

We ensure that the interelement jumps $[\![v]\!]$ are constrained to be zero by using a Lagrange multiplier μ, and that leads to a introduction of the Lagrange functional Λ defined by,

$$\begin{aligned} &\Lambda: V(\wp) \times \Xi \to R \\ &\Lambda(v, \mu) = J_\wp(v) - \mu([[\, v]]) \end{aligned} \tag{33}$$

where, the Ξ denotes the space of Lagrange multipliers. From Eqs. (32) and (33),

$$\begin{aligned} \Lambda(v, \mu) &= \sum_{K=1}^{N(\wp)} \left\{ \Pi_K(v) - \Pi_K(u^{q,h}) - \int_{\partial\Omega_K \setminus \partial\Omega} v^T \langle \Gamma(n)\, \sigma(u^{q,h})\rangle_{1-\alpha} ds \right\} \\ &\quad - \mu([[\, v]]) + \sum_{\Gamma_{KL}} \int_{\Gamma_{KL}} [[\, v^T]] \langle \Gamma(n)\, \sigma(u^{q,h})\rangle_{1-\alpha} ds \end{aligned} \tag{34}$$

This functional is composed of sum of local contributions from each element Ω_K and extra coupled terms from each interelement boundary Γ_{KL}. But, if we take $\mu = \widehat{\mu}$, then Λ becomes a sum of

$$\widehat{\mu}([[\, v]]) = \sum_{\Gamma_{KL}} \int_{\Gamma_{KL}} [[\, v^T]] \langle \Gamma(n)\, \sigma(u^{q,h})\rangle_{1-\alpha} ds \tag{35}$$

purely uncoupled local contributions.

Using the relation of Eq. (31), we notice that, for any $v \in V(\Omega)$, $\Lambda(v, \mu) = J(v)$. Then from Eq. (26),

$$-\frac{1}{2}\| e \|_E^2 = J(u) = inf_{v \in V(\Omega)} \Lambda(v, \mu) \tag{36}$$

Now, let us define the functional $\Phi: V(\wp) \rightarrow \overline{R}$ as $\Phi(v) = \sup_{\mu \in \Xi} \Lambda(v, \mu)$, then it shows that

$$\Phi(v) = \begin{cases} J(v), & v \in V(\Omega) \\ +\infty, & v \notin V(\Omega) \end{cases} \tag{37}$$

and $2 \inf_{v \in V(\wp)} \Phi(v) = 2 \inf_{v \in V(\Omega)} \Phi(v) = \| e \|_E^2$. Moreover

$$\begin{aligned} inf_{v \in V(\Omega)} J(v) &= inf_{v \in V(\wp)} sup_{\mu \in \Xi} \Lambda(v, \mu) \\ &\geq sup_{\mu \in \Xi} inf_{v \in V(\wp)} \Lambda(v, \mu) \\ &\geq inf_{v \in V(\wp)} \Lambda(v, \widehat{\mu}), \quad \forall \widehat{\mu} \in \Xi \end{aligned} \tag{38}$$

With the choice of a Lagrange multiplier $\widehat{\mu}$ in Eq. (35), an upper bound of the global error is given below:

$$\| e \|_E^2 \leq -2 \sum_{K=1}^{N(\wp)} inf_{v \in V_K} \left\{ \Pi_K(v) - \Pi_K(u^{q,h}) - \int_{\partial\Omega_K \setminus \partial\Omega} v^T \langle T(n_K)\, \sigma(u^{q,h}) \rangle_{1-\alpha} ds \right\} \tag{39}$$

Since the second term in Eq. (39) computed from the finite element approximate solution $u^{q,h}$ is invariant, we need only to solve the following local element-wise variational problems:

$$\begin{aligned} &\text{Find } \widehat{u}_K \in V_K \text{ such that } \forall v \in V_K \\ &a_K(\widehat{u}_K, v) = \ell_K(v) + \int_{\partial\Omega_K \setminus \partial\Omega} v^T \langle T(n_K)\, \sigma(u^{q,h}) \rangle_{1-\alpha} ds \end{aligned} \tag{40}$$

Obviously, equilibrated local problems are defined on three-dimensional broken spaces V_K. With this $\widehat{u}_K$, Eq. (39) becomes

$$\begin{aligned} &-2\, inf_{v \in V_K} \left\{ \Pi_K(v) - \Pi_K(u^{q,h}) - \int_{\partial\Omega_K \setminus \partial\Omega} v^T \langle T(n_K)\, \sigma(u^{q,h}) \rangle_{1-\alpha} ds \right\} \\ &= a_K(\widehat{u}_K, \widehat{u}_K) + 2\Pi_K(u^{q,h}) \\ &= a_K(\widehat{u}_K - u^{q,h}, \widehat{u}_K - u^{q,h}) + \int_{\partial\Omega_K \setminus \partial\Omega} u^{q,h^T} \langle T(n_K)\, \sigma(u^{q,h}) \rangle_{1-\alpha} ds \end{aligned} \tag{41}$$

and from the fact of $[[\, u^{q,h}]] = 0$, Eq. (41) results in:

$$\begin{aligned} \| e \|_E^2 &\leq a_K(\widehat{u}_K - u^{q,h}, \widehat{u}_K - u^{q,h}) + \sum_{K>L}^{N(\wp)} \int_{\Gamma_{KL}} [[\, u^{q,h^T}]] \langle T(n_K)\, \sigma(u^{q,h}) \rangle_{1-\alpha} ds \\ &= a_K(\widehat{u}_K - u^{q,h}, \widehat{u}_K - u^{q,h}) \end{aligned} \tag{42}$$

By denoting $a_K(\widehat{u}_K - u^{q,h}, \widehat{u}_K - u^{q,h})$ as η_K^2, we finally have

$$\| e \|_E^2 \leq \sum_{K=1}^{N(\wp)} \eta_K^2 \tag{43}$$

The quantity η_K is thus error indicator in the element Ω_K and contributes to the global error

bound.

Next, consider the discretization of the local element-wise problem (40) by introducing the local finite element approximation solution space $V_K^h = V^{q,h}$ as a restriction of the initial finite element approximation space $V^{q,h}(\Omega)$ in Eq. (19) to the element Ω_K with higher p_K and q_K. Then, the corresponding discrete local element-wise problem is:

$$\text{Find } \hat{u}_K^h \in V_K^h \text{ such that } \forall\, v^h \in V_K^h$$
$$a_K(\hat{u}_K^h,\, v^h) = \ell_K(v^h) + \int_{\partial\Omega_K \setminus \partial\Omega} v^{h^T} \langle\, T(n_K)\, \sigma(u^{q,h}) \rangle_{1-\alpha} ds \Big\} \tag{44}$$

And then, $(\eta_K^h)^2 = a_K(\hat{u}_K^h - u^{q,h},\, \hat{u}_K^h - u^{q,h}) \approx (\eta_K)^2$.

Calculation of Self-Equilibrating Fluxes

Here, we introduce the local flux splitting and equilibration method of Ainsworth and Oden (1993). Finite element approximations of hierarchical models are two-dimensional, but the flux splitting on interelement boundaries is three-dimensional. Let $F(\mathcal{S})$ denote the set of all vertices in the partition, and consider any vertex $A \in F(\mathcal{S})$. Associated with each such vertex node A is a piecewise trilinear shape function $\psi_A(x)$, which vanishes at every other vertex node in this partition and has a unit value at the node A. With this shape function, the flux splitting function $\alpha_{KL}(s)$ of Eq. (29) is expressed on the interelement face Γ_{KL} which has four end nodes; A,B,C and D:

$$\alpha^k_{KL}(s) = \sum_{N=A}^{D} \alpha^k_{KL}(s)\, \psi_N(s), \quad k = 1,2,3 \tag{45}$$

Now, return to the local weak formulation of a single element $K \in \mathcal{S}$ with a sufficiently smooth vector-valued test function $\phi(x)$ on the element K. If we take $\phi = (1,1,1)^T$,

$$a_K(u,\, 1) = \ell_K(1) + \int_{\partial\Omega_K \setminus \partial\Omega} 1^T T(n)\, \sigma(u)\, ds \tag{46}$$

Eq. (46) characterizes the equilibration of an element Ω_K, and its solution is the restriction of true solution u to the element Ω_K, $u|_{\Omega_K}$. If we replace u in Eq. (46) with the initial finite element approximate solution $u^{q,h}$ and rewrite the above equation for each component of the test function $1 = 1^1 + 1^2 + 1^3 = \{(1,0,0) + (0,1,0) + (0,0,1)\}^T$, then Eq. (47) represents the compatibility

$$a_K(u^{q,h},\, 1^k) = \ell_K(1^k) + \int_{\partial\Omega_K \setminus \partial\Omega} \langle\, T(n)\, \sigma(u^{q,h}) \rangle^k_{1-\alpha} ds \tag{47}$$

condition on the k-interelement traction component $\langle \cdot \rangle^k_{1-\alpha}$ for the existence of local solution.

Since $u^{q,h}$ is given from the initial finite approximation, compatibility condition imply to find splitting factors α^k_{KL} for the self-equilibrated traction component that makes the element Ω_K be in force equilibrium in the k-direction.

If we consider the difference, RHS-LHS in Eq. (47), then which means the lack in the force equilibrium in the k-direction on Ω_K and we denote it by Δ^k_K. Because the trilinear shape function $\psi_A(x)$ has the following property,

$$\sum_{A \in F(\mathcal{S})} \psi^1_A(x) = (1,0,0)^T, \quad \forall\, x \in \Omega \tag{48}$$

the lack $\triangle_K^k$ of force equilibrium in the k-direction is expressed in terms of shape functions.

$$\begin{aligned} \triangle_K^k &= \sum_{A \in \mathcal{T}(\mathcal{S})} \triangle_{K,A}^k \\ \triangle_{K,A}^k &= \ell_K(\psi_A^k) + \int_{\partial\Omega_K \setminus \partial\Omega} \psi_A^k \langle \Gamma(n)\, \sigma(u^{q,k}) \rangle_{1-\alpha}^k ds - a_K(u^{q,k}, \psi_A^k) \end{aligned} \tag{49}$$

The above equation has significant importance of the fact that flux splitting problem coupled with the elements in the patch $F(\mathcal{S})$ of the node A becomes the decoupled problem for each node A.

For computational convenience, we introduce an anti-symmetric operator $x_{KL}: \Gamma_{KL} \to R$,

$$x_{KL}^k = \alpha_{KL}^k - 1/2 \;\Rightarrow\; x_{KL}^k + x_{LK}^k = 0 \tag{50}$$

then, using these new quantities, we have the following relations from Eqs. (30) and (50):

$$\begin{aligned} \langle \Gamma(n)\, \sigma(u^{q,k}) \rangle_{1-\alpha}^k &= \frac{1}{2} \langle \Gamma(n)\, \sigma(u_K^{q,k}) + \Gamma(n)\, \sigma(u_L^{q,k}) \rangle^k \\ &= \langle \Gamma(n)\, \sigma(u^{q,k}) \rangle_{1/2}^k + x_{LK}^k [[\, \Gamma(n)\, \sigma(u^{q,k})]]^k \end{aligned} \tag{51}$$

With further definition of the following two quantities using the above relations,

$$\begin{aligned} b_{K,A}^k &= \ell_K(\psi_A^k) + \int_{\partial\Omega_K \setminus \partial\Omega} \psi_A^k \langle \Gamma(n)\, \sigma(u^{q,k}) \rangle_{1/2}^k ds - a_K(u^{q,k}, \psi_A^k) \\ \rho_{LK,A}^k &= -\int_{\Gamma_{KL}} \psi_A^k [[\, \Gamma(n)\, \sigma(u^{q,k})]]^k ds \end{aligned} \tag{52}$$

Eq. (49) becomes

$$\begin{aligned} \triangle_{K,A}^k &= b_{K,A}^k - \sum_{L>0} x_{LK,A}^k \rho_{LK,A}^k \\ &= b_{K,A}^k - \sum_{L>0} \hat{x}_{LK,A}^k \end{aligned} \tag{53}$$

Then, $\hat{x}_{LK}^k = -\hat{x}_{KL}^k$ because x_{LK}^k is anti-symmetric and $\rho_{LK,A}^k$ is symmetric. We will use $\hat{x}_{LK}^k$ for L > K; then the vanishing of $\triangle_{K,L}^k$ is equivalent to write

$$\sum_{L>K>0} \hat{x}_{LK}^k - \sum_{K>L>0} \hat{x}_{KL}^k = b_{K,A}^k \tag{54}$$

Now, consider a patch of elements sharing the common node A denoted by

$$\mathcal{T}_A = \{ \cup \Omega_K \subset \Omega \mid \Omega_K \text{ supp } (\psi_A) \} \tag{55}$$

Then, we construct a system of equations such as Eq. (56) for the elements in the patch of the node A. Consequently, we can split equilibrated fluxes on interelement boundaries with respect to each node by solving the following linear equations,

$$M_A \hat{x}_A^k = b_A^k, \quad k = 1,2,3, \quad \forall A \in F(\mathcal{S}) \tag{56}$$

with.

$$b_A^k = \{b^k_{K_1,A}, b^k_{K_2,A}, \cdots, b^k_{K_{Aed},A}\}^T$$
$$\hat{x}_A^k = \{\hat{x}^k_{LK}, \cdots\}^T, \quad L>K \tag{57}$$

Here, M_A is the $N_{Ael} \times N_{Aed}$ underlying matrix for a patch consisting of N_{Ael} elements and N_{Aed} interelement faces sharing common node A.

After solving the linear system of equations, we compute flux splitting factors α^k_{KL} through the relation of Eq. (50), and calculate self-equilibrated tractions $\langle \cdot \rangle_{1-\alpha}$ on interelement boundaries. Finally, with the computed self-equilibrated tractions, we solve the local variational problems defined in Eq. (44) to get better approximate solutions $\hat{u}^h_K$ which are being used for estimating error indicators.

Numerical Experiments

Fig. 2 shows a clamped square plate-like body with uniform thickness. Uniformly distributed traction t_z is applied on the top surface. From the symmetry, only a quarter of the body is taken for numerical analysis. Data used for the analysis are: $E=10^7 N/m^2$, $\nu=0.3$, $a=1.0\,m$ and $t_z=5.0\times10^{-4} N/m^2$.

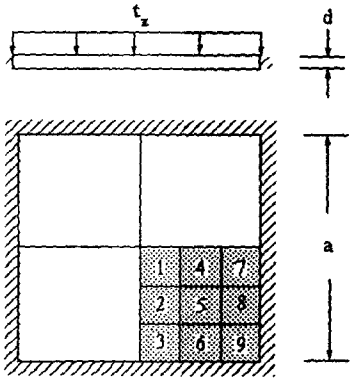

Fig. 2 A square plate-like structure subjected to uniform normal traction (a/d=20)

We use the (1,1,0)* hierarchical model and uniform 9 quadratic elements. Vertical displacement component is shown in Fig. 3, where "DOM" indicates the ratio (or called the bending dominance) of bending strain energy to total strain energy calculated from the approximated solution. The finite element simulation was carried out using hpq-adaptive finite element CODE developed by the first author, which is fully automatic program capable of systematic selection of the optimal model and the optimal finite element mesh to meet the predefined analysis tolerance.

In order to evaluate the quality of the proposed error estimator, the effectivity index θ is computed. Since the exact analytic solution for this problem is not available, we use the approximated

$$\theta = \text{Estimated error / Exact error} \tag{58}$$

solution u_{ref} using relatively higher model and higher approximation orders with the same mesh partition (here, we use q=(8,8,8) and p=8). With this alternative choice, we compute local and

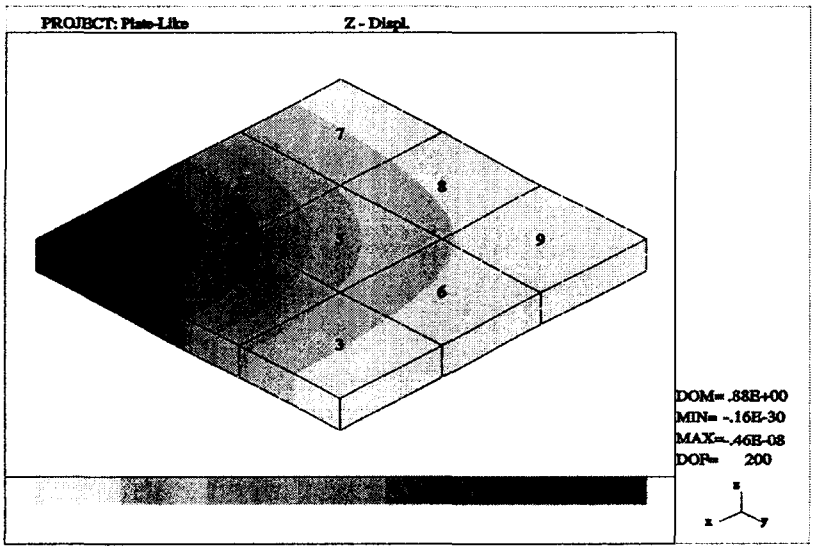

Fig. 3 Spectral distribution of vertical displacement component (p=2, q=(1,1,0)*)

global effectivity index θ_K, θ defined by

$$\theta_K = \eta_K^h / \eta_K \approx \| \widehat{u}_K^h - u^{q,h} \|_{E(\Omega_K)} / \| u_{ref} - u^{q,h} \|_{E(\Omega_K)}$$
$$\theta = \left\{ \sum_{K=1}^{N(S)} \theta_K^2 \right\}^{1/2} \approx \| \widehat{u}_K^h - u^{q,h} \|_{E(\Omega)} / \| u_{ref} - u^{q,h} \|_{E(\Omega)} \quad (59)$$

Table. 1 contains results of estimation of local and global error indicators and effectivity indices, and shows comparison with the conventional error estimator which simply splits interelement fluxes by half ($\alpha_{KL}=1/2$). Numerical results show that local error indices of the proposed method are considerably improved and more evenly distributed.

Table. 1 Estimated error and effectivity index for plate-like structure

Elem. No.	Error (E-7)			Effectivity Index	
	True	With Equil.	Without Equil.	With Equil.	Without Equil.
1	0.85307	0.87095	0.88607	1.02096	1.03868
2	0.53854	0.66702	0.81643	1.23855	1.51599
3	0.97427	0.99747	1.04193	1.02381	1.06944
4	0.53854	0.66702	0.81643	1.23855	1.51599
5	0.35162	0.54995	0.70580	1.56403	2.00726
6	0.66379	0.64317	0.75346	0.96894	1.13509
7	0.97427	0.99747	1.04193	1.02381	1.06944
8	0.66379	0.64317	0.75346	0.96894	1.13509
9	0.35837	0.31199	0.38437	0.87059	1.07255
Total	2.08314	2.20576	2.46389	1.05886	1.18278

Next, we consider a cylindrical roof supported by two diaphragms, a representative engineering example, as shown in Fig. 4. By a diaphragm support is meant $u_r = u_\theta = 0$, and loading is due to its own weight γ. The same material with the previous plate-like body is selected, and the other data are L=5m, R=1m and γ=4.0N/m^3. Using the symmetry of the body, numerical analysis was done by applying the (1,1,0)* hierarchical model and uniform 9 quadratic elements to a quarter.

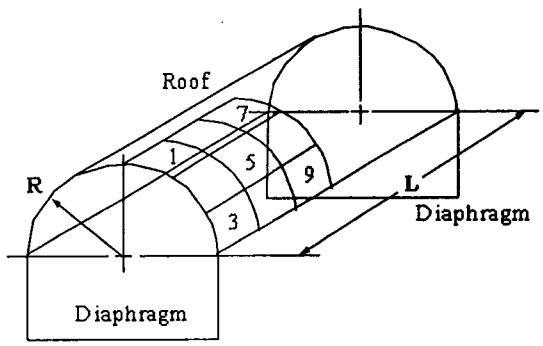

Fig. 4 A cylindrical roof supported by vertical diaphragms (R/d=20)

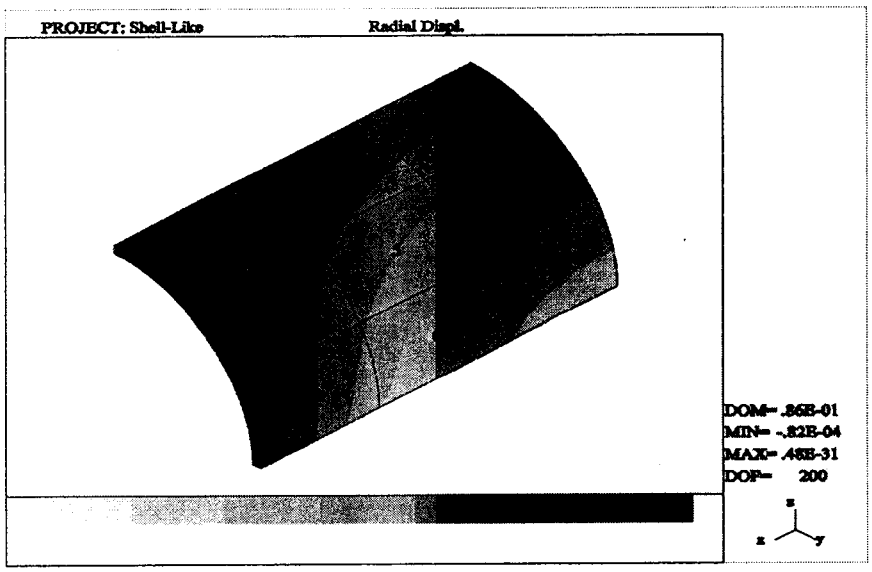

Fig. 5 Spectral distribution of radial displacement component (p=2, q=(1,1,0)*)

Fig. 5 depicts the radial displacement component, where we can find out from the value of "DOM" that this problem is not bending-dominated. And since the real radial displacement component is opposite to the radial direction, its magnitude is negative in the figure.

Table. 2 Estimated error and effectivity index for shell-like structure

Elem. No.	Error (E-3)			Effectivity Index	
	True	With Equil.	Without Equil.	With Equil.	Without Equil.
1	0.31097	0.32848	0.46491	1.05630	1.49503
2	0.29901	0.37936	0.52926	1.26875	1.77007
3	0.43736	0.48229	0.48249	1.10273	1.10318
4	0.66185	0.75400	1.09591	1.13924	1.65583
5	0.43974	0.61942	1.07351	1.40861	2.44123
6	0.76130	0.67162	0.70302	0.88220	0.92345
7	0.86592	0.91143	1.35222	1.05256	1.56160
8	0.53236	0.53972	1.19800	1.01044	2.25037
9	0.95932	0.76257	0.81017	0.79490	0.84452
Total	1.88199	1.89454	2.73803	1.00666	1.45486

Following the same procedure to estimate error indicators and effectivity indices, we obtain the numerical results presented in Table. 2. We can see the improvement in the shell-like problems, too. In particular, big deviation in the conventional method is reported in the elements 5 and 8, while acceptable values are obtained with the proposed method.

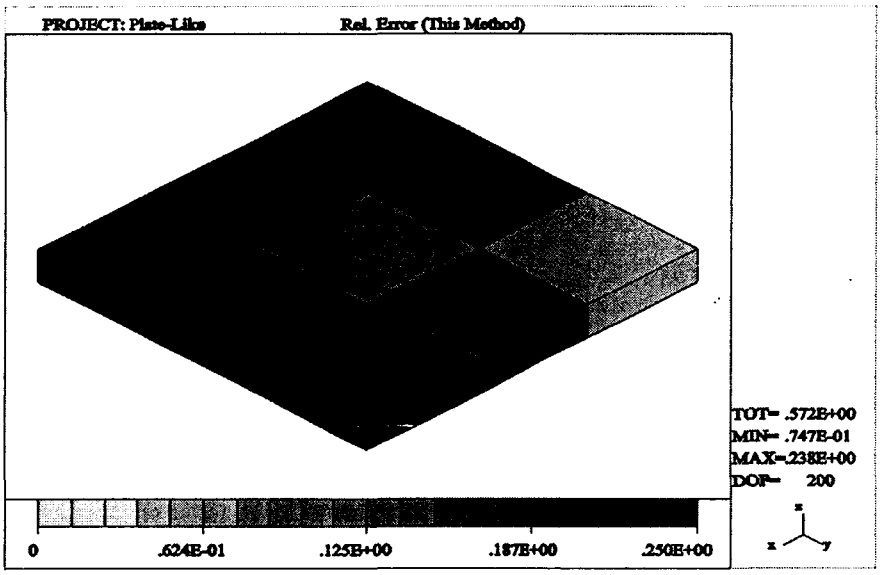

Fig. 6 Distribution of local relative errors (p=2, q=(1,1,0)*)

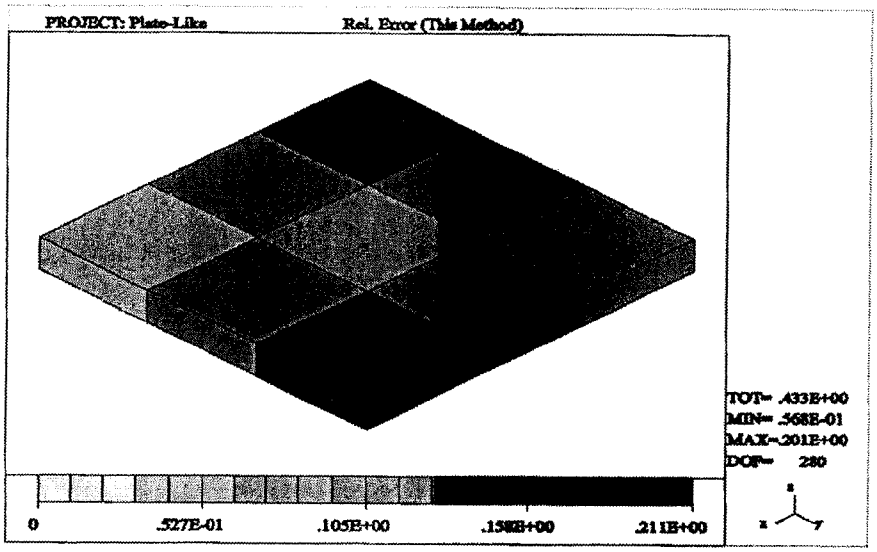

Fig. 7 Distribution of local relative errors (p=2, q=(1,1,2))

The above Fig. 6 shows a distribution of local relative errors obtained by the proposed method. Here, relative error is defined by $\eta_K^h / U(u^{q,h})$. From the figure, the global relative error is 57.2% of total strain energy, and major contribution is come from the elements 1,3 and 7. It is interesting for the element 1 to have big error, however this phenomenon disappears if the (1,1,2) hierarchical model, the next higher model by one, is used, as shown in Fig. 7.

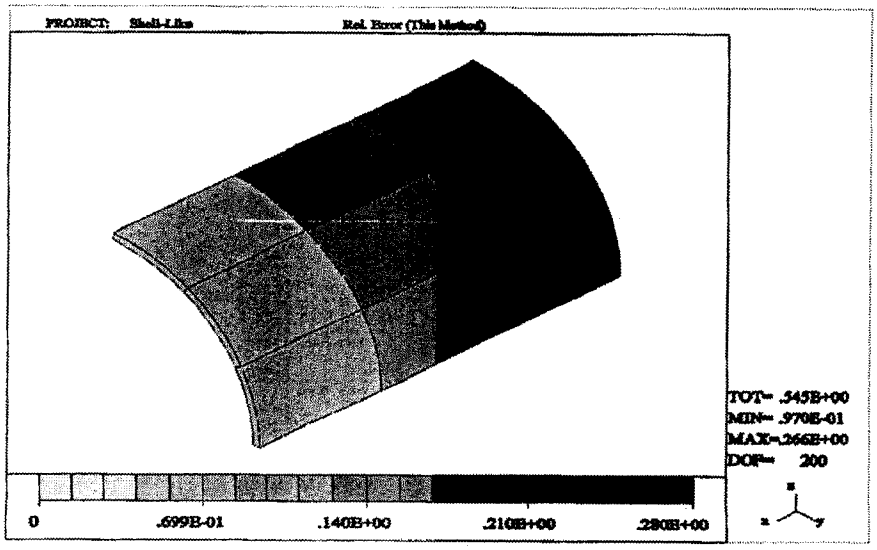

Fig. 8 Distribution of local relative errors (p=2, q=(1,1,0)+)

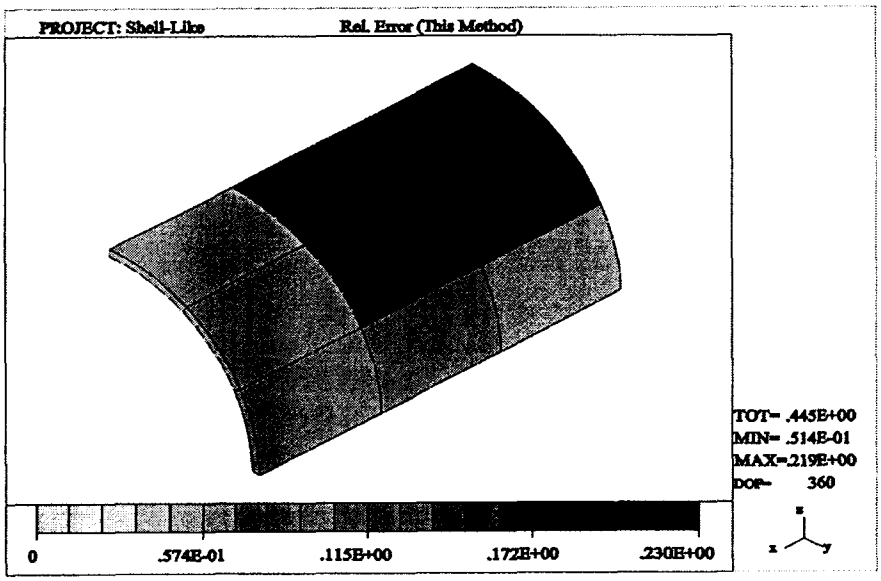

Fig. 9 Distribution of local relative errors (p=2, q=(2,2,2))

Figs. 8 and 9 represent distribution of local relative errors when the (1,1,0)* and the (2,2,2) hierarchical models, respectively, are employed for the approximation. A decrease in the global relative error from 54.5% to 44.5% indicates that the proposed error estimator successfully measures the modeling error component.

Conclusions and Discussion

In this paper, with a brief introduction of the concept of hierarchical models, we derived an a posteriori error estimator for hierarchical models for elastic structures with thin domains such as plate- and shell-like structures, and which can measure the total error with respect to the three-dimensional linear elasticity theory. In the development of the proposed error estimator, flux splitting technique for element-wise force equilibrium and Lagrange multiplier method are employed. In order to approximate the exact solution, we use self-equilibrated interelement tractions and solve the localized finite element problem using higher model levels and higher approximation orders.

From the two representative model problems, theoretical arguments underlying the development have been verified. Compared to the conventional error estimator which splitts interelement fluxes by half, better effectivity indices uniformly distributed over the elements have been obtained.

With this tool, the analyst can estimate his numerical quality and further he can control model levels, mesh sizes and approximation orders in order to enhance the accuracy. Then, the quality assurance and time saving can be achieved.

Here, a question is "can we apply the same theoretical results to other types of hierarchical models with different key parameters being used to determine the model level ?". Among other types of problems may be the analysis of phase composite bodies, general fluid flows, inelastic bodies, etc. Still, there has not been remarkable studies on this point, however one invariant core is to develope techniques capable of obtaining the solution of the highest model in each type of problems.

References

Adams, R. A., 1978, *Sobolev Spaces*, Academic Press Inc.

Ainsworth, M. and Oden, J. T., 1993, "A Unified Approach to *A Posteriori* Error Estimation using Element Residual Methods," *Numer. Math.*, Vol. 65, pp. 23-50.

Babuska, I. and Li, L., 1992, "The Problem of Plate Modeling : Theoretical and Computational Results," *Comp. Meth. Appl. Mech. Eng.*, Vol. 100, pp. 249-273.

Babuska, I., Szabo, B. A., and Actis, R. L., 1992, "Hierarchical Models for Laminated Composites," *Numer. Meth. Eng.*, Vol. 33, pp. 503-535.

Cho, J. R. and Oden, J. T., 1996, "*A Priori* Modeling Error Estimates of Hierarchical Models for Elasticity Problems for Plate- and Shell-Like Structures," *Mathl. Comput. Modelling*, Vol. 23, No. 10, pp. 117-133.

Cho, J. R. and Oden, J. T., 1996, "*A Priori* Error Estimations of *hp*-Finite Element Approximations for Hierarchical Models of Plate- and Shell-Like Structures," *Comp. Meth. Appl. Mech.*, Vol. 132, pp. 135-177.

Ciarlet, P. G., 1978, *The Finite Element Method for Elliptic Problems*, North-Holland, Amsterdam.

Noor, A. K. and Burton, W. S., and Peters, J. M., 1992, "Hierarchical Adaptive Modeling of Structural Sandwiches and Multilayered Composite Panels," A. K. Noor ed., AMD - Vol. 157, ASME Publications, pp. 47-67.

Oden, J. T. and Cho, J. R. 1996, "Adaptive *hpq*-Finite Element Methods of Hierarchical Models for Plate- and Shell-Like Structures," *Comp. Meth. Appl. Mech. Eng.*, Vol. 136, pp. 317-345.

Oden, J. T., Demkowicz, L., and Westermann, T. A., 1989, "Towards a Universal *h-p* Adaptive Finite Element Strategy, Part 2. *A Posteriori* Error Estimation, *Comp. Meth. Appl. Mech. Eng.*, Vol. 77, pp. 113-180.

Reddy, J. N., 1984, "A Simple Higher-Order Theory for Laminated Composite Plates," *J. Appl. Mech.*, ASME, Vol. 51, PP. 745-752.

Schwab, C., 1996, "*A Posteriori* Modelling Error Estimation for Hierarchic Plate Models," *Numer. Math.*, Vol. 74, No. 2, pp. 221-259.

Szabo, B. A. and Babuska, I., 1991, *Finite Element Analysis*, John Wiley, N.Y..

Szabo, B. A. and Sahrmann, G. J., 1988, "Hierarchic Plate and Shell Models Based On *p*-Extensions," *Numer. Meth. Eng.*, Vol. 26, pp. 1855-1881.

Vogelius, M. and Babuska, I., 1981, "On a Dimensional Reduction Method; I. The Optimal Selection of Basis Functions," *Math. Comp.*, Vol. 37, No. 156, pp. 361-384.

Wempner, G., 1973, *Mechanics of Solids with Applications to Thin Bodies*, McGraw-Hill.

Zienkiwicz, O. C. and Zhu, J. G., 1987, "A Simple Error Estimator and Adaptive Procedure for Practical Engineering Analysis," *Numer. Meth. Eng.*, Vol. 24, pp. 337-357.